J Supercond Nov Magn (2016) 29:2075–2084
DOI 10.1007/s10948-016-3516-0

ORIGINAL PAPER

The Structural, Magnetic, and Magnetocaloric Properties of $La_{1-x}Ag_xMnO_3$ ($0.05 \leq x \leq 0.25$)

A. Coşkun[1,2] · E. Taşarkuyu[1,2] · A. E. Irmak[1,2] · S. Aktürk[1,2] · A. Ekicibil[3]

Received: 17 December 2015 / Accepted: 13 April 2016 / Published online: 23 April 2016

Abstract We have investigated structural, magnetic, and magnetocaloric properties of monovalent Ag-doped $La_{1-x}Ag_xMnO_3$ ($0.05 \leq x \leq 0.25$) compounds. The materials were prepared by the sol–gel method and then characterized by X-ray diffraction (XRD). The XRD results indicated that all the samples have a single phase of hexagonal (rhombohedral) structure with the $R\bar{3}c$ space group. The morphology and particle size distributions were investigated using scanning electron microscopy (SEM) with energy-dispersive spectroscopy (EDS). The SEM images showed that the grain sizes are smaller than 1 μm and remain the same with increasing Ag concentrations. The magnetic properties were studied by measuring magnetization and varying temperature ($M(T)$) and external magnetic field ($M(H)$). The $M(T)$ measurements show that with decreasing temperature all samples exhibit a paramagnetic-to-ferromagnetic phase transition. The Curie temperature, T_C, increases from 200 to 290 K as Ag doping increases from 0.05 to 0.25. The magnetic entropy change ($|-SM|$) is obtained in all samples near the Curie temperatures at a magnetic field change of 3 T. Furthermore, their maximum relative cooling power (RCP) values were found to be 82.492, 82.614, and 127.375 J/kg for $x = 0.10$, 0.15, and 0.25.

Keywords Manganite · Sol-gel · Magnetic entropy change · Curie temperature

1 Introduction

Perovskite rare earth (RE) manganites are doped with bivalent or monovalent cations $RE_{1-x}A_xMnO_{3+\delta}$ (where RE is a rare earth cation and A is a doping cation). They have been intensively studied over the last decade. Many attempts have sought the doping providing the highest sensitivity of the electrical resistivity to the magnetic field at the room temperature. This is the most important challenge for the application of manganites as magnetic field sensors or movement sensors and magnetic cooling applications. Magnetic cooling systems have high efficiency and are used in scientific and technological purposes at very low temperatures below room temperature. There has been an increase in research on the magnetocaloric effect (MCE) of manganite-based materials, due to the possibility of applying this effect for magnetic refrigeration close to room temperature [1–5]. In the chemical form of $La_{1-x}A_xMnO_3$, A is a monovalent ion such as Na, Li, Ag, and K or a divalent ion such as Ca, Sr, Ba, and Pb. It has exhibited a large MCE around room temperature [6, 7]. These compounds exhibit large enough magnetic entropy change (ΔS_M), which is a measure of MCE and paramagnetic–ferromagnetic phase transition temperature (T_C = Curie temperature). The low production costs, good chemical stability, tunable ordering temperature, ease of giving a form, and low magnetic hysteresis are among the other advantages of these compounds. It is well known from the literature that the physical

✉ A. Coşkun
coskunatilla@gmail.com

[1] Department of Physics, Faculty of Sciences, Mugla Sitki Kocman University, 48000 Mugla, Turkey

[2] Magnetic Materials Laboratory, Research Laboratory Center, Mugla Sitki Kocman University, 48000 Mugla, Turkey

[3] Department of Physics, Faculty of Sciences, Çukurova University, 01330, Adana, Turkey

properties, such as T_C, ΔS_M, and adiabatic temperature change (ΔT_{ad}), can be tuned in a wide range depending on the oxidation state of the dopant, ionic radius of the dopant, and doping concentration level [8–10]. However, for these materials to be used as active magnetic cooling elements for room temperature applications, all parameters must be optimized. This has not been achieved. $LaMnO_3$ has a perovskite structure with antiferromagnetic-insulator properties. However, substitution of lanthanum by a small amount of monovalent or divalent element gives rise to enormous changes in magnetic and electrical properties of the compounds [11, 12]. On the other hand, these materials can show different electronic and magnetic properties due to the preparation techniques and the thermal process. In the literature, many series of different monovalent dopants at A-site substituted materials have been reported [13–15]. However, it should not be noted that the large magnetic entropy changes are induced by low magnetic field changes at room temperature. Tang et al. have prepared $La_{1-x}Ag_xMnO_3$ ($x = 0.05, 0.20, 0.25, 0.30$) compounds by using the solid-state reaction method [16]. They found that the T_C values 214, 278, 306, and 306 K increase as Ag concentration increases. The higher maximum magnetic entropy change value was found to be 3.4 J/kgK at 278 K for $x = 0.20$. S. Das et al. found that the T_C values increase (260, 287, and 309 K) with the increase in K doping for the $La_{1-x}K_xMnO_3$ ($x = 0.05, 0.10$, and 0.15) samples which were prepared by pyrophoric technique [17]. They calculated the maximum entropy change values are 2.73, 2.73, and 3 J/kgK upon a magnetic field change of 1 T. L.K. Lakshmi et al. prepared monovalent substituted lanthanum manganites $La_{0.67}A_{0.33}MnO_3$ ($A = Li^{1+}$, Na^{1+}, K^{1+}, and Rb^{1+}) by sol-gel route by sintering at 1200 °C. They calculated the T_C values are 146, 315, 243, and 195 K for the Li^{1+}, Na^{1+}, K^{1+}, and Rb^{1+} doping, respectively [18]. M. Koubaa et al. synthesized the $La_{0.65}Ca_{0.35-x}Na_xMnO_3$

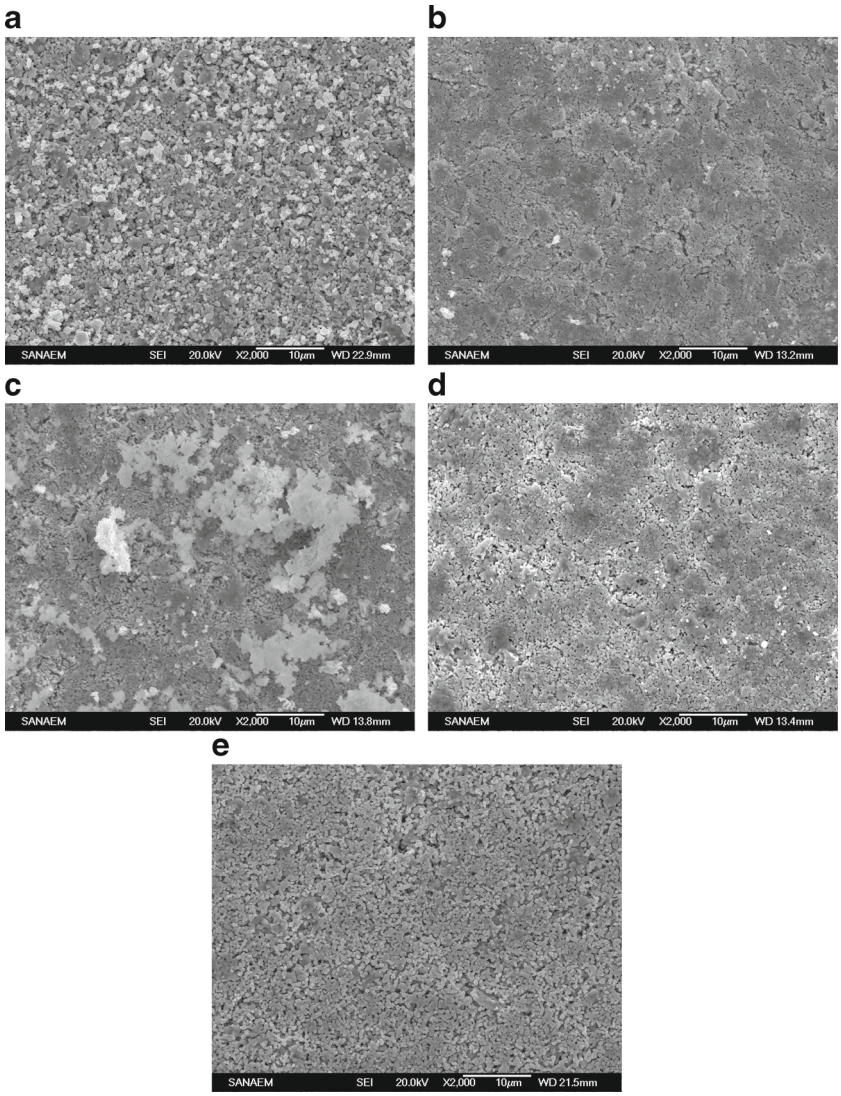

Fig. 1 SEM images of (**a**) $La_{0.95}Ag_{0.05}MnO_3$, (**b**) $La_{0.90}Ag_{0.10}MnO_3$, (**c**) $La_{0.85}Ag_{0.15}MnO_3$, (**d**) $La_{0.80}Ag_{0.20}MnO_3$, and (**e**) $La_{0.75}Ag_{0.25}MnO_3$ compounds

($0 \leq x \leq 0.25$) samples by the solid-state method, and they investigated the effect of Na doping on the structural, magnetic, and magnetocaloric properties of these materials [19].

It is clearly seen that from the above studies, paramagnetic-to-ferromagnetic transition temperature and magnetic entropy change are highly sensitive to the doping concentration, preparation techniques and sintering temperature, and ionic radii of dopant ions. The size of the substitutional ion and its concentration in the A site play important roles in the magnetic properties of these manganites. The partial substitution of La by other elements with a larger/smaller ionic radius such as Na, K, Ba, and Pb produces the structural disorder in MnO_6 octahedra, modifying the Mn–O–Mn bond length and bond angles and Mn^{3+}/Mn^{4+} ratio, and results in changing lattice and electronic properties. It seems like the study of $LaMnO_3$-based manganites is necessary to work. The effect of other monovalent dopants still has been waiting better study, in particular that of the silver doping.

In this paper, in order to optimize T_C and ΔS_M, we substituted La by a monovalent Ag element, taking into account the known effects of the heat treatment process on the magnetic properties. For this aim, $La_{1-x}Ag_xMnO_3$ ($x = 0.05$, 0.10, 0.15, 0.20, and 0.25) compounds were prepared by sol-gel route for homogeneity of the samples. It was known that Ag can segregate easily at the grain boundary at a high sintering temperature higher than 1000 °C [20]. So, the prepared samples have been heat treated at 1000 °C for 24 h. The morphological and crystallographic properties of the samples have been investigated by scanning electron microscopy (SEM-EDS) and x-ray diffraction (XRD) techniques. The magnetic properties have been explored by the physical properties measurement system (PPMS). From these analyses, relations of the structural and the crystallographic properties with magnetic properties have been established with the help of known theories for possible contribution to the theoretical studies.

2 Experimental Procedure

The polycrystalline samples of the $La_{1-x}Ag_xMnO_3$ ($x = 0.05$, 0.10, 0.15, 0.20, and 0.25) were prepared by sol-gel method. Appropriate amounts of La_2O_3, $Ag(NO_3)_2$, and $Mn(NO_3)_2$ with desired stoichiometries were dissolved in dilute HNO_3 solution at 150 °C. Then, citric acid and ethylene glycol were added to the mixture. Viscous residual was formed by slowly boiling this solution at 200 °C. The obtained residual was dried slowly at 300 °C until dry-gel was formed. Finally, the residual precursor was burned in air at 600 °C in order to remove organic materials produced during chemical reactions. The material obtained from this

Table 1 Actual and nominal compositions for $La_{1-x}Ag_xMnO_3$ ($0.05 \leq x \leq 0.25$) compounds

Ag concentration	0.05	0.10	0.15	0.20	0.25
Actual composition	$La_{0.95}Ag_{0.05}MnO_3$	$La_{0.90}Ag_{0.10}MnO_3$	$La_{0.85}Ag_{0.15}MnO_3$	$La_{0.80}Ag_{0.20}MnO_3$	$La_{0.75}Ag_{0.25}MnO_3$
Nominal composition	$La_{0.95}Ag_{0.045}MnO_3$	$La_{0.90}Ag_{0.96}MnO_3$	$La_{0.85}Ag_{0.12}MnO_3$ metalic Ag	$La_{0.80}Ag_{0.15}MnO_3$ metalic Ag	$La_{0.75}Ag_{0.17}MnO_3$ metalic Ag

process was ground to a fine powder by using an agate mortar. The pellets were produced from each composition by pressing into 13-mm radii and 2-mm thicknesses under a pressure of 3 tons. Each pellet set was then separately sintered at 1000 °C for 24 h in air and cooled down to room temperature in the furnace.

SEM investigations were performed using a JEOL SEM 7700F, equipped with an EDS system. XRD was performed ($10° \leq 2\theta \leq 70°$) using a Bruker D8 Advance X-Ray Diffractometer with a CuKα_1 radiation. The magnetic properties were measured using a Quantum Design PPMS with a closed cycle helium cryostat from 10 to 340 K with magnetic fields up to 5 T. From the temperature dependence of magnetization, T_C values were determined at an applied field of 100 Oe. In order to determine the magnetocaloric characteristics, $M(H)$ measurements were made around T_C from $H = 0$ to 5 T at constant temperatures and, at each set of measurements, the temperature was changed with steps of 3 K for both increasing and decreasing values.

3 Results and Discussion

The surface morphology and grain size of the $La_{1-x}Ag_xMnO_3$ ($0.05 \leq x \leq 0.25$) manganite compounds were investigated with SEM as shown in Fig. 1a–e. From the SEM images, it is apparent that the sizes, distributions, and morphologies of the grain remain nearly the same with increasing Ag concentration for all samples. The surface morphologies of the samples have small grain sizes which are not formed in a closely packed condition (<1 μm) and also contain some porosities. This is most probably because the sintering temperature was not high enough to obtain good crystallized samples. The relation between the nominal and the actual compositions has been determined by EDS technique through general analyses over low magnified images. In order to obtain the compositions of the samples accurately, the EDS analyses have been made by averaging the data gathered from distinct locations of the samples. For doping concentrations less than $x = 0.15$, there are minor differences between the nominal and the actual concentrations for all samples (Table 1). However, above $x = 0.15$, Ag losses become significant in the perovskite structure. There are also possibilities in which some Ag is in metallic form and the rest of the Ag is in the perovskite phase.

The XRD patterns of $La_{1-x}Ag_xMnO_3$ ($0.05 \leq x \leq 0.25$) compounds are shown in Fig. 2. It is noticeable that the patterns consist of only the peaks of hexagonal structure belonging to $R\bar{3}c$ and without any other secondary or impurity phases for the $La_{1-x}Ag_xMnO_3$ ($x = 0.05$ and 0.10) samples. However, for concentration values of $x = 0.15$, 0.20, and 0.25, characteristic peaks belonging to metallic Ag are observed at $2\theta = 38°$.

Figure 3a–e shows the magnetizations of the compounds as a function of temperature measured in a field 100 Oe for the temperature region from 4 to 320 K, in both field-cooled (FC) and zero field-cooled (ZFC) modes. The curves are denoted by ZFC and FC, respectively. It is seen that from Fig. 3, the ZFC and FC curves have similar temperature dependences, and all samples exhibit a ferromagnetic-paramagnetic transition. However, there is a split between the ZFC and FC curves of the samples near the T_C. This thermomagnetic irreversibility may be due to the intrinsic

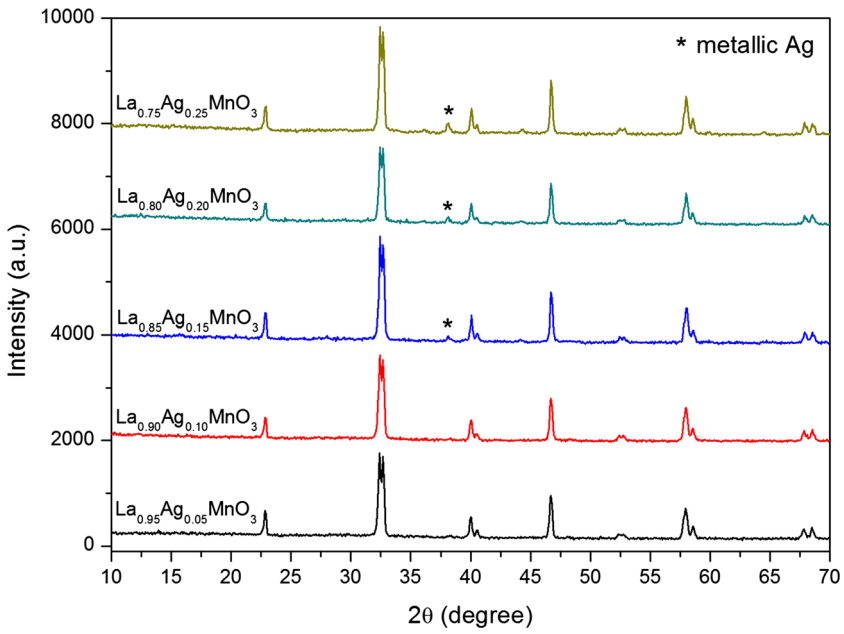

Fig. 2 The XRD pattern of $La_{1-x}Ag_xMnO_3$ ($0.05 \leq x \leq 0.25$) compounds

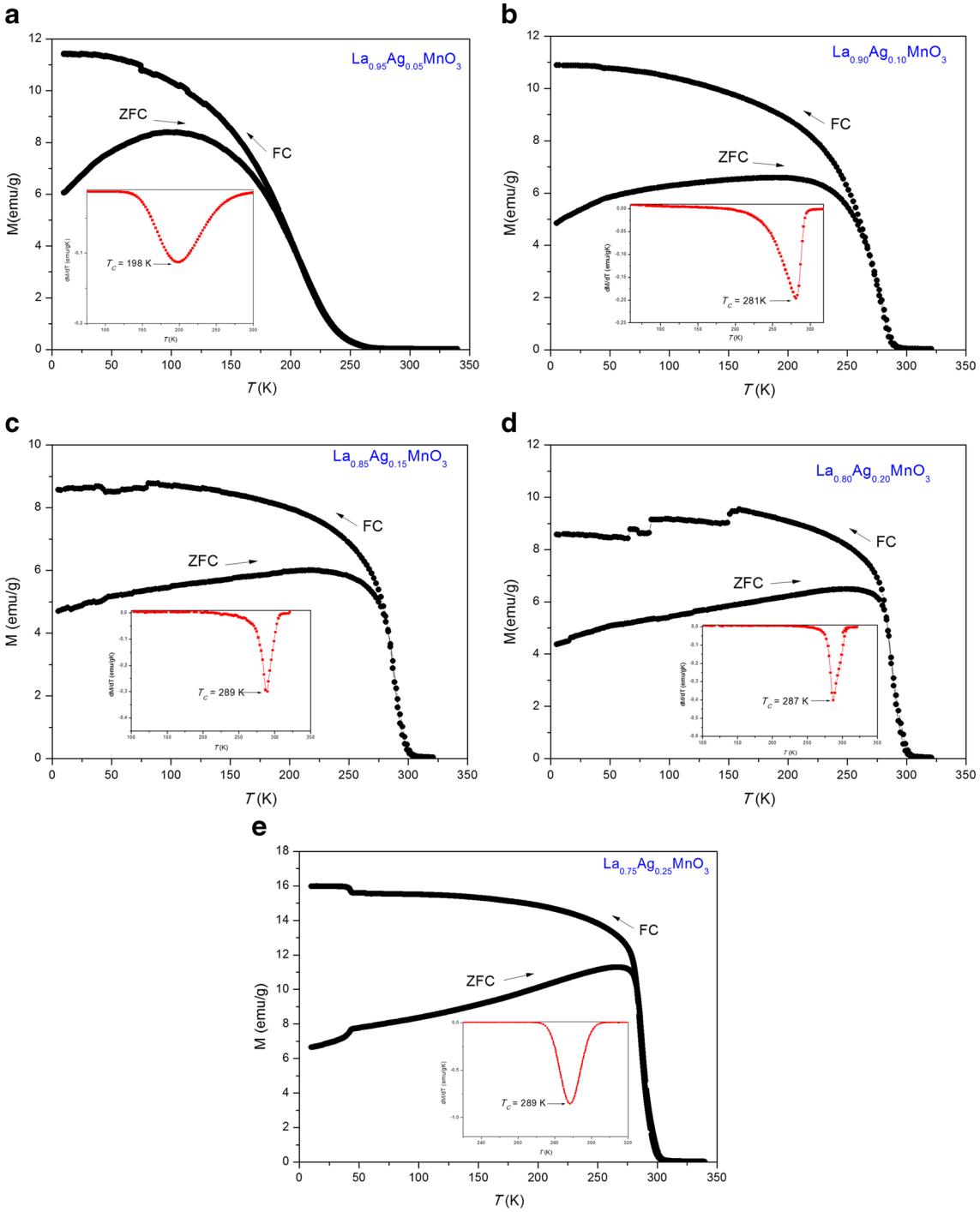

Fig. 3 The temperature dependence of magnetization measured at magnetic field 100 Oe for (**a**) $La_{0.95}Ag_{0.05}MnO_3$, (**b**) $La_{0.90}Ag_{0.10}MnO_3$, (**c**) $La_{0.85}Ag_{0.15}MnO_3$, (**d**) $La_{0.80}Ag_{0.20}MnO_3$, and (**e**) $La_{0.75}Ag_{0.25}MnO_3$ compounds (the *inset* is the plot of dM/dT vs. T)

magnetic anisotropy and to domain wall pinning effect in the magnetically ordered state. The ZFC curves lie somewhat lower than the FC curves. The lower-lying character of the ZFC curves is attributed to a more random frozen magnetic configuration than achieved in the FC cases [21]. The point where *dM/dT* reaches the minimum determines T_C is maximum on the magnetization curve shift to higher values with the increase in the Ag content (x = 0.05, 0.10, 0.15, 0.20, and 0.25), and T_C values are 198, 281, 289, 287, and 289 K, respectively, which is of room temperature. The increase in the T_C value takes place due to the oxidation of Mn^{3+} ions into Mn^{4+} ions with the increase

of Ag doping concentration as it is known; $LaMnO_3$ has a perovskite structure with antiferromagnetic properties. However, substitution of lanthanum by a small amount of monovalent element gives rise to immense changes in magnetic properties of the compound. As a result of monovalent ion substitution of La^{3+} ions, it oxidizes two Mn^{3+} ions to two Mn^{4+} ions proportional to the amount of monovalent ion. It is well known that Mn^{3+} and Mn^{4+} ions differ in their ionic radii. La^{3+} and the substitute ion may also have different ionic radii. Because of these ionic radii differences, the concentration level plays a very important part in the crystal structure of the resulting compound. Depending on the increase in Ag concentration, the number of Mn^{4+} ions increases and the ratio of the Mn^{3+}/Mn^{4+} decreases in the compounds. The increase in the number of Mn^{4+} ions in the structure yields a rise in the number

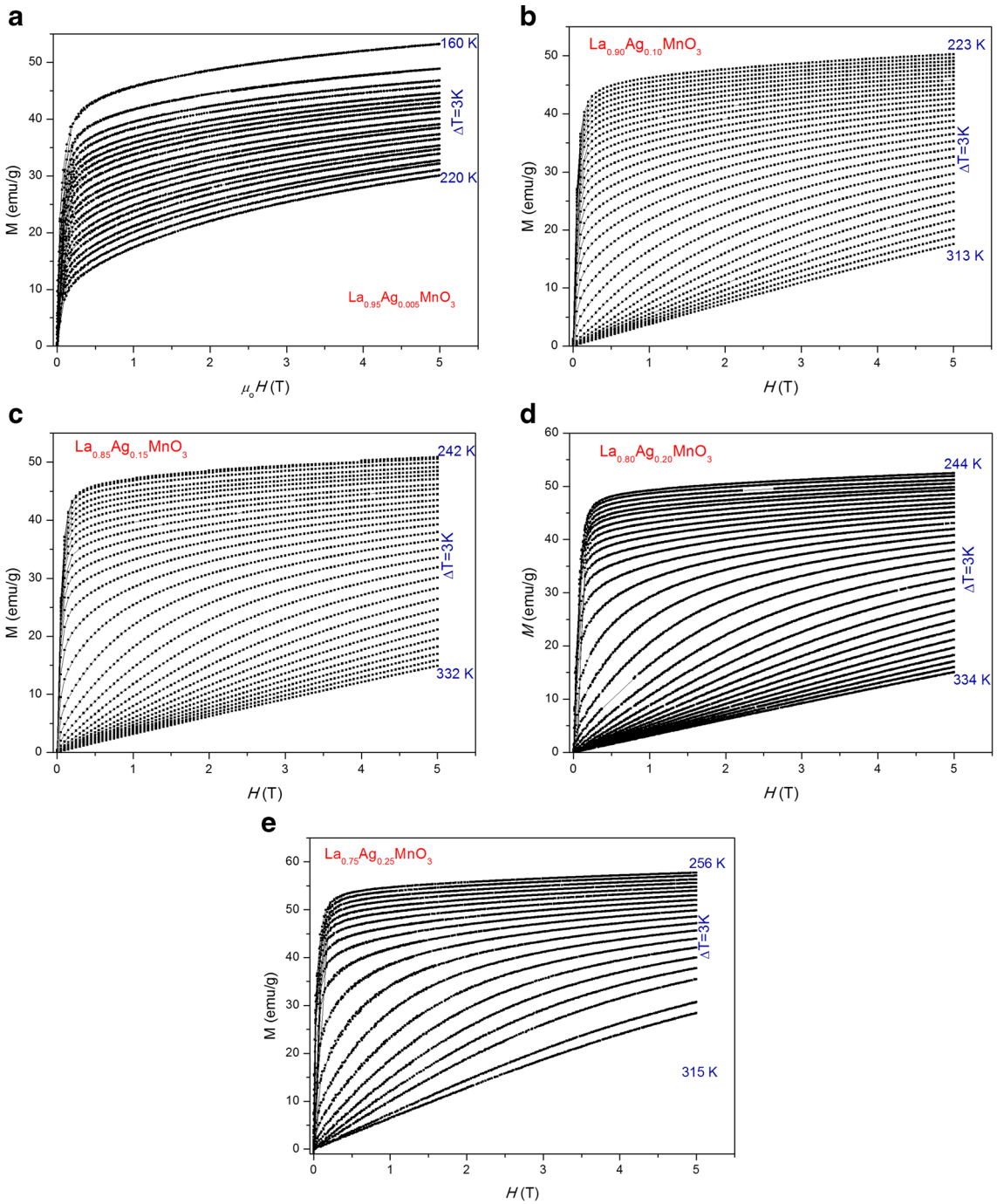

Fig. 4 $M(H)$ curves of (**a**) $La_{0.95}Ag_{0.05}MnO_3$, (**b**) $La_{0.90}Ag_{0.10}MnO_3$, (**c**) $La_{0.85}Ag_{0.15}MnO_3$, (**d**) $La_{0.80}Ag_{0.20}MnO_3$, and (**e**) $La_{0.75}Ag_{0.25}MnO_3$ compounds near T_C

of Mn^{3+}–O^{2-}–Mn^{4+} pairs resulting in greater numbers of double-exchange interactions. The double-exchange mechanism is effective directly on the ferro-paramagnetic phase transition. The region of transition is broader for the least doped sample and becomes steeper with the increase of doping concentration. The steepness or broadness of the transition region may stem from a few factors, one being the grain size. A smaller grain size gives a larger proportion of surface near-spins which may be weaker ferromagnetically coupled than spins in the bulk of the grains. This could give a distribution of Curie temperature and thus a broadened magnetic transition. The double-exchange interaction is weaker on the surface than in the body of grains. The grain boundaries between the adjacent grains behave as potential barriers effecting magnetic properties that weaken ferromagnetism [22]. Another factor for the shape

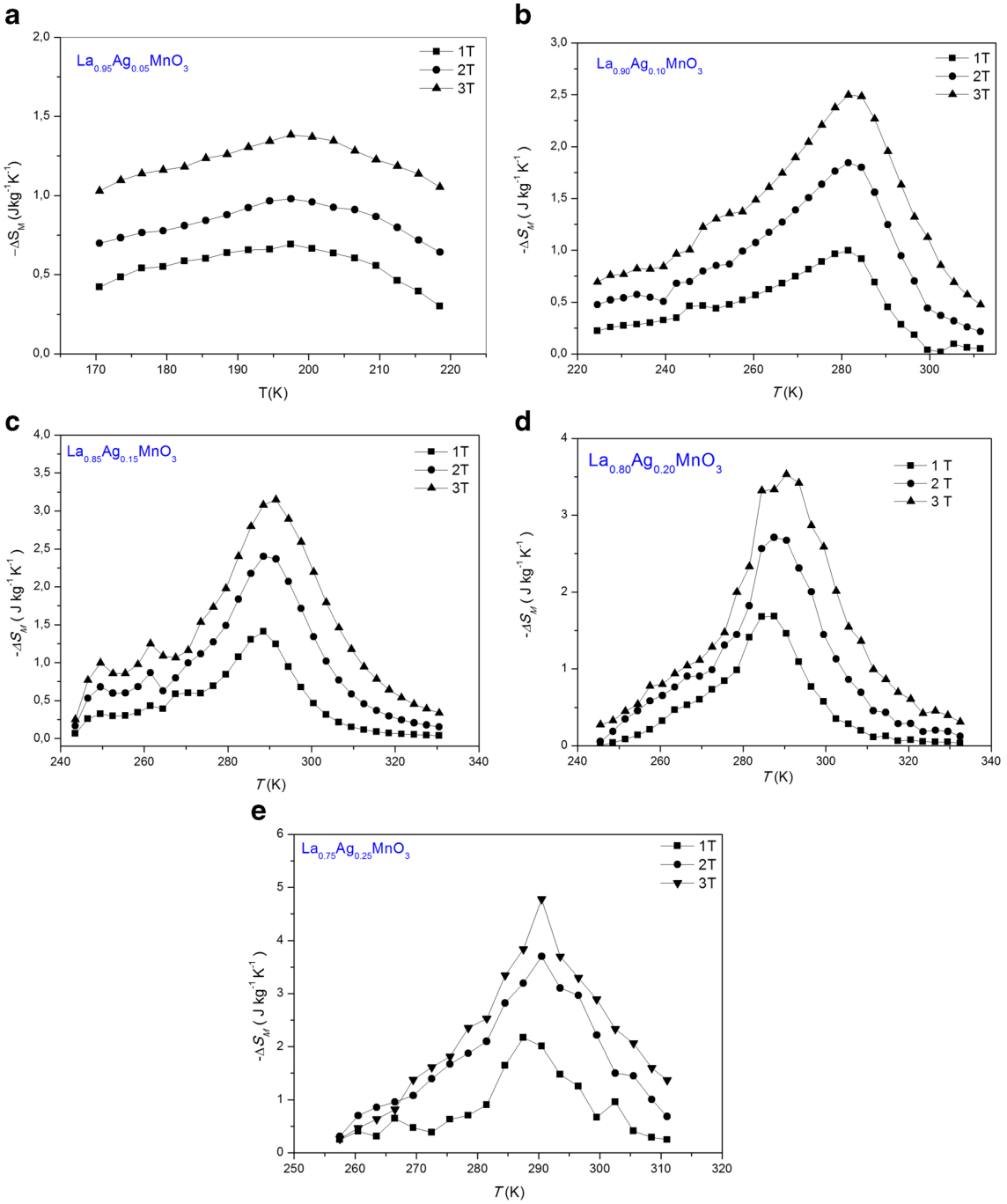

Fig. 5 The temperature dependence of ΔS_M for (**a**) $La_{0.95}Ag_{0.05}MnO_3$, (**b**) $La_{0.90}Ag_{0.10}MnO_3$, (**c**) $La_{0.85}Ag_{0.15}MnO_3$, (**d**) $La_{0.80}Ag_{0.20}MnO_3$, and (**e**) $La_{0.75}Ag_{0.25}MnO_3$ compounds

(steepness/broadness) of the transition region would be due to the deviation of oxygen stoichiometry. It is possible to speculate that the broadness of the transition region of the least doped sample would be evidence for the deviation of oxygen stoichiometry [23].

The magnetization vs. applied field, $M - H$, and curves of the samples were taken with 3K intervals both below and above the Curie temperature of the samples with respect to the external applied magnetic fields up to 5 T. Figure 4a, b shows the isothermal magnetization curves for all samples. To investigate the effect of Ag substitution on the magnetic entropy change of the compound, we have calculated the magnetic entropy change, ΔS_{M}. The magnetic entropy change induced by the variation of the external magnetic field from 0 to maximum field H is given by

$$\Delta S_{\mathrm{M}}(T)_{H,P} = \int (\partial M(T, H)/\partial T)_{H,P} dH$$

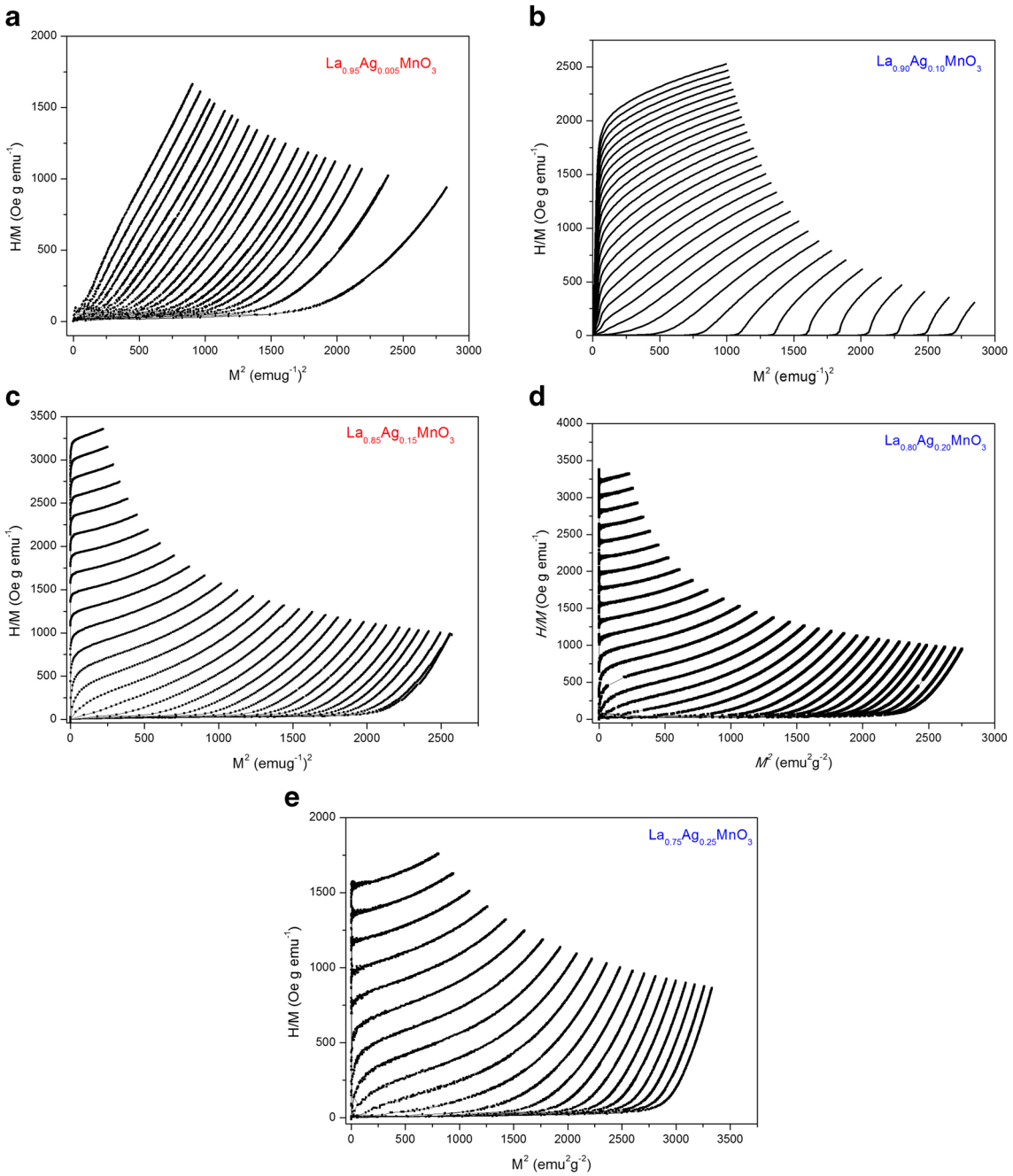

Fig. 6 The Arrott plots of (**a**) $La_{0.95}Ag_{0.05}MnO_3$, (**b**) $La_{0.90}Ag_{0.10}MnO_3$, (**c**) $La_{0.85}Ag_{0.15}MnO_3$, (**d**) $La_{0.80}Ag_{0.20}MnO_3$, and (**e**) $La_{0.75}Ag_{0.25}MnO_3$ compounds near T_C

Utilizing the discrete form of the above equation and the $M - H$ curves allow us to calculate the absolute value of magnetic entropy change ($|\Delta S_M|$) for each sample as shown in Fig. 5a–e. The maximum of the magnetic entropy change curves coincides nearly with the Curie temperatures of the corresponding samples. The magnetic entropy change observed in the perovskite manganites is related with the change of the magnetization around the Curie temperature. The maximum magnetic entropy change occurs for the sample with $x = 0.25$, and it is calculated to be 4.8 J/kg/K for 3 T.

Additionally, the increase in the doping concentration makes these $|\Delta S_M|$ curves steeper. The increase in $|\Delta S_M|$ with the increase of doping concentration can be explained by the double-exchange mechanism. The ferromagnetic double exchange (Mn^{3+}–O^{2-}–Mn^{+4}) dominates over the antiferromagnetic super exchange (Mn^{3+}–O^{2-}–Mn^{3+}/Mn^{4+}–$O^{2--}Mn^{4+}$) due to the increase of doping concentration. This is not only due to the oxidation state of the ions replaced by La ions but also their average ionic radii. The average ionic radius of A and B sites has an impact on the lattice parameters of the perovskite structure. The average A site ionic radius, r_A, increased from 1.2192 to 1.2320 Å and the average ionic radius of the B site, r_B, decreases from 0.6335 to 0.5875 Å due to the increase in Ag concentration. Spin-lattice coupling occurring during magnetic ordering is another factor affecting the magnetic entropy. Because magnetic change in manganite is due to the spin-lattice couplings, Mn–O bond length and Mn–O–Mn bond angle will be changed depending on the temperature and, consequently, will cause a volumetric change that will contribute to the ranking of spins [24, 25].

In order to determine the degree of the magnetic transition in samples, Arrott plots (H/M vs. M^2) which were converted from the isothermal M–H data are shown in Fig. 6a–e for the $La_{1-x}Ag_xMnO_3$ series. According to the criterion proposed by Banerjee [26], a negative or positive sign of the slope of the H/M vs. M^2 curves corresponds to a first-order or second-order magnetic phase transition, respectively. As shown in Fig. 6a–e, all samples show a positive slope confirming that a second-order FM to PM phase transition occurs. The relative cooling power (RCP) is expressed with the following equation: $RCP(S) = (-\Delta S_M)_{max}(T, H) \times \delta T_{FWHM}$; here, $(-\Delta S_M)_{max}$ is the maximum entropy change and δT_{FWHM} is the temperature difference at the half maximum of that change. The RCP values of the samples are given in Table 2.

Table 2 The RCP values for $La_{1-x}Ag_xMnO_3$ ($x = 0.10, 0.15, 0.25$) compounds

Composition	RCP (Jkg^{-1})		
	1T	2T	3T
x = 0.10	27.299	53.468	82.492
x = 0.15	31.692	58.057	82.614
x = 0.25	29.642	80.051	127.375

4 Conclusion

In summary, the structural and the magnetic properties of Ag-doped $LaMnO_3$ perovskite compounds were investigated. XRD analysis revealed that the crystal structure of the samples belong to the $R\bar{3}c$ space group with orthorhombic symmetry. It was also determined that excess metallic Ag accumulates in the structure when doping concentration is above 0.15. The samples in this work were prepared by sol-gel technique and heated at 600 °C, giving powdery compounds. The Ag oxides used in the sol-gel dissolve as oxide and metallic Ag above 300 °C. This is the reason that the XRD patterns of the samples with $x \geq 0.15$ contain the trace of metallic Ag. One of them might be to consider different preparation techniques such as solid-state reaction, and the other might be to use more Ag than is required in nominal stoichiometry. Using both solid-state reaction and sealed quartz tubes to hold the compound material for heat treatment may result that Ag ions are kept in the structure with desired stoichiometric ratio. The large difference in valencies of La^{3+} and Ag^{1+} ions and the random distribution of Ag^{1+} ions in the A site and the crystal structure are probably causing the magnetic inhomogeneity. It is found that the Curie temperatures shifted to (higher temperatures) room temperature with the increase of Ag doping level. From magnetization measurements, $|\Delta S_M|_{max}$ was found to be 4.8 J/kgK for $x = 0.25$ at 3 T. Furthermore, their maximum relative cooling power (RCP) values were found for $x = 0.10$, 0.15, and 0.25 as 82.492, 82.614, and 127.375 J/kg, respectively.

References

1. Cheikh-Rouhou Koubaa, W., Koubaa, M., Cheikhrouhou, A.: J. Alloys Compd. **453**, 42–48 (2008)
2. Pekała, M., Drozd, V.: J. Alloys Compd. **456**, 30–33 (2008)
3. Bejar, M., Dhahri, E., Hlil, E.K., Heniti, S.: J. Alloys Compd. **440**, 36–42 (2007)
4. Zhang, J.-Q., Lia, N., Feng, M., Pan, B.-C., Li, H.-B.: J. Alloys Compd. **467**, 88–90 (2009)
5. Liang, L., Hui, X., Zhang, C.M., Chen, G.L.: J. Alloys Compd. **463**, 30–33 (2008)
6. Samancıoğlu, Y., Coşkun, A.: J. Alloys Compd. **507**, 380–385 (2010)
7. Luong, N.H., Hanh, D.T., Chau, N., Tho, N.D., Hiep, T.D.: J. Magn. Magn. Mater. **290–291**, 690–693 (2005)
8. Srivastava, S.K., Kar, M., Ravi, S.: J. Magn. Magn. Mater. **320**, e107–e110 (2008)

9. Wang, Z.M., Tang, T., Wang, Y.P., Zhang, S.Y., Du, Y.W.: J. Magn. Magn. Mater. **246**, 254–258 (2002)
10. Huang, S., Cui, X., Wang, D., Han, Z., Du, Y.: J. Alloys Compd. **398**, 184–187 (2005)
11. Lina, G.C., Weib, Q., Zhang, J.X.: J. Magn. Magn. Mater. **300**, 392–396 (2006)
12. Koubaa, M., Cheikhrouhou-Koubaa, W., Cheikhrouhou, A., Ranno, L.: Physica B **403**, 4012–4019 (2008)
13. Kamilov, I.K., Gamzatov, A.G., Aliev, A.M., Batdalov, A.B., Aliverdiev, A.A., Abdulvagidov, S.B., Melnikov, O.V., Gorbenko, O.Y., Kaul, A.R.: J. Phys. D: Appl. Phys. **40**, 4413–4417 (2007)
14. Hien, N.T., Thuy, N.P.: Physica B **319**, 168–173 (2002)
15. Jian, W.: J. Alloys Compd. **476**, 859–863 (2009)
16. Tang, T., Gu, K.M., Cao, Q.Q., Wang, D.H., Zhang, S.Y., Du, Y.W.: J. Magn. Magn. Mater. **222**, 110–114 (2000)
17. Das, S., Dey, T.K.: J. Alloys Compd. **440**, 30–35 (2007)
18. Lakshmi, L.K., Venkataiah, G., Vithal, M., Reddy, P.V.: Physica B **403**, 3059–3066 (2008)
19. Joseph Joy, V.L., Joy, P.A., Date, S.K.: Appl. Phys. Lett. **78**, 3747 (2001)
20. Irmak, A.E., Coskun, A., Tasarkuyu, E., Akturk, S., Unlu, G., Samancıoglu, Y., Sarikurkcu, C., Kaynar, B.M., Yucel, A.: J. Magn. Magn. Mater. **322**, 945–951 (2010)
21. Joy, P.A., Kumar, P.S.A., Date, S.K.: J. Phys. Condens. Matter **10**, 11049–11054 (1998)
22. Koubaaa, M., Cheikhrouhou-Koubaaa, W., Cheikhrouhoua, A., Haghiri-Gosne, A.M.: Physica B **403**, 2477–2483 (2008)
23. Zhang, N.: Phys. Rev. B **56**(13), 8138–8142 (1997)
24. Ju, H.L., Gopalakrishnan, J., Peng, J.L., Li, Q., Xiong, G.C., Venkatesan, T., Greene, R.L.: Phys. Rev. B **51**(9), 6143–6146 (1995)
25. Radelli, P.G., Coe, D.E., Marezio, M., Cheong, S.W., Schiffer, P.E., Ramirez, A.P.: Phys. Rev. Lett **75**, 4488 (1995)
26. Banerjee, B.K.: Phys. Lett. **12**, 16 (1964)